Fine Chemical Engineering
http://ojs.wiserpub.com/index.php/FCE/

Research Article

Preparation of Value-added Chemicals via Chemical Looping Pyrolysis of Corn Straws with Ca-Fe Composite Oxygen Carrier

Wenyao Li, Longxin Zhao, Xiao He, Jingjing Liu, Yongzhuo Liu*, Qingjie Guo

Laboratory of Green & Smart Chemical Engineering in Universities of Shandong, College of Chemical Engineering, Qingdao University of Science and Technology, Qingdao, P. R. China
Email: yzliu@qust.edu.cn

Received: 22 April 2024; **Revised:** 11 June 2024; **Accepted:** 14 June 2024

Abstract: Biomass chemical looping pyrolysis (BCLPy), which utilizes either reduced or oxidized oxygen carriers for biomass pyrolysis, enables the simultaneous production of high-quality bio-oils and clean syngas. In this study, CLPy of corn straws with a Ca-Fe composite oxygen carrier was investigated to produce value-added chemicals by optimizing both temperature and the mass ratio of oxygen carrier to biomass (OC/B). It has been demonstrated that the reduced Ca-Fe oxygen carrier (Re-OC) promotes hydrocarbon formation and facilitates removal of oxygenated compounds from bio-oils. Under optimal conditions (Re-OC/B = 4:3, T = 650 °C), the relative percentage of benzene, toluene and xylene (BTX) in the bio-oil reaches 27.0 area%, while that of 2-pentenone accounts for 38.0 area% at 550 °C with a Re-OC/B mass ratio of 1:3. The maximum yield based on corn straws approaches 4.7 wt.%. Regarding the oxidized Ca-Fe oxygen carrier (Ox-OC), the relative percentage of 2,3-dihydrobenzofuran (2,3-DHB) reaches a maximum value of 11.6 area% at 600 °C with an Ox-OC/B mass ratio of 2:3. Under catalytic ketonization of $Ca_2Fe_2O_5$ oxygen carrier, a maximum value of 28.0 area% is achieved with an Ox-OC/B mass ratio of 4:3 at 450 °C. In summary, BCLPy provides a completely new strategy for producing biomass-derived chemicals with added value.

Graphical abstract

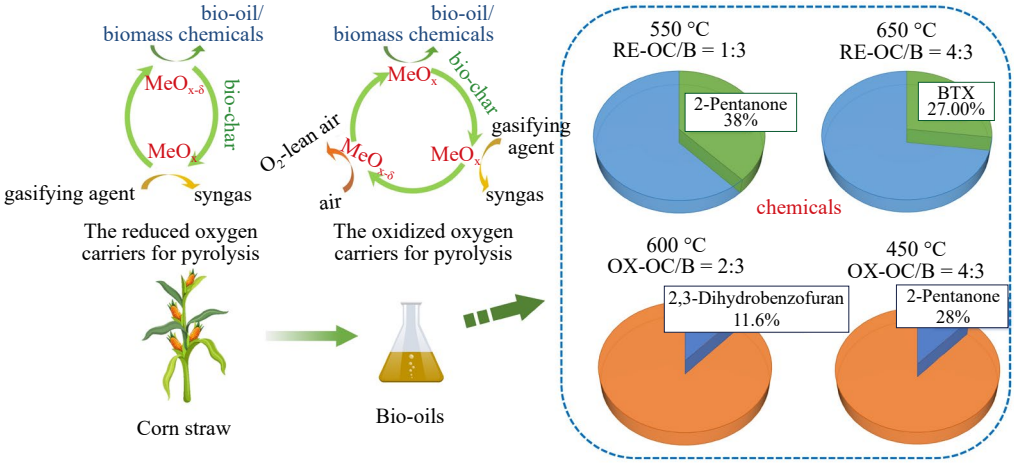

DOI: https://doi.org/10.37256/fce.5220244794

***Keywords*:** corn straws, chemical looping pyrolysis, BTX, 2-pentanone, 2,3-dihydrobenzofuran

1. Introduction

Biomass is a crucial form of clean and renewable energy, playing a significant role in mitigating the energy crisis and addressing environmental pollution issues.[1] Given China's status as an agricultural country, it possesses a substantial theoretical resource potential of 977 million tons of straws by 2022. Moreover, corn, being a vital food crop with extensive cultivation areas and short growth cycles, results in approximately 340 million tons of corn straw waste due to open burning and random dumping. These unsustainable practices not only contribute to increasing greenhouse gas emissions but also exacerbate environmental problems while squandering valuable resources.[2] Consequently, there has been growing attention towards the recycling and utilization of renewable resources derived from corn straw through advancements in biochemical technology and energy science.[3]

The conversion of biomass into biofuels, chemicals, and carbon materials through thermochemical and biochemical methods offers a significant resolution to energy and environmental challenges.[4-6] Among thermochemical techniques, pyrolysis enables the simultaneous production of high-value products such as combustible gas, bio-oil, and bio-char. This facilitates the classified and staged utilization of biomass, representing a crucial research direction and hotspot for the high-value utilization of biomass.[7-9] However, direct pyrolysis-derived bio-oil often faces challenges including complex composition, elevated oxygen content, heightened acidity, and limited stability. In order to enhance the quality of pyrolysis products, in-situ upgrading methods such as catalytic pyrolysis, hydropyrolysis, and co-pyrolysis are proposed along with ex-situ upgrading method, i.e. catalytic deoxygenation of the generated bio-oils.[10-12]

Catalytic pyrolysis not only enables the generation of biofuel with high calorific value such as clean gas, biodiesel, and jet-fuel, but also facilitates the production of value-added chemicals, including L-glucosone, acetone, hydroxymethylfurfural, phenols, and aromatic hydrocarbons.[13-20] Many of these compounds are challenging to synthesize using conventional chemical methods. Reported catalysts for biomass pyrolysis encompass metal oxides and molecular sieves, including ZrO_2, Al_2O_3, CaO, CeO_2 and ZSM-5.[21-25] Chaihad et al. reported that catalytic HZSM-5 molecular sieve-assisted pyrolysis significantly reduces oxygen-containing compounds (e.g., ketones phenols acids) in bio-oil.[26] Che et al observed higher benzene, toluene and xylene (BTX) yields in products using Zn-modified zeolite.[27] Li et al. investigated co-catalytic pyrolysis of low-density polyethylene and cellulose and found that when their mass ratio was 1:4, actual aromatics yield increased by 39.3% compared to theoretical values.[28] However, challenges persist regarding carbon loss, hydrogen consumption, and catalyst inactivation which reduce the atom economy of carbon/hydrogen utilization and limit catalyst recycling.

In order to address the aforementioned issues, Liu et al. proposed a novel biomass pyrolysis method called chemical looping pyrolysis (CLPy), which utilizes an oxygen carrier to decouple biomass thermal conversion into a two-stage reaction at different temperatures.[29-30] Two schemes can be employed to implement this method, i.e. catalytic pyrolysis using reduced oxygen carriers and oxidized oxygen carriers, respectively. He et al. synthesized six types of iron-based oxygen carriers by incorporating alkaline earth metals (Ca, Sr, Ba) and transition metals (Co, Ni, Cu) as secondary components respectively.[31] Experimental investigations on corn stalk biomass demonstrated that these six reduced oxygen carriers significantly reduce the content of oxygen compounds in bio-oil while promoting the formation of hydrocarbons. In the presence of Ca-Fe oxygen carrier, the content of carboxylic acid compounds notably decreases from 29.4 area% to 0.3 area%, while CO yield reaches 330 L/kg biomass during the semi-coke gasification stage. Furthermore, Ca-Fe oxygen carrier exhibited excellent catalytic activity as well as redox properties after ten cycles. With microalgae biomass as feedstock, the mass fraction of oxygen in bio-oil decreases from 37.6% without oxygen carrier to 12.7% with the reduced Ca-Fe oxygen carrier, while the content of heptadecone and benzene in bio-oil increased to 18.8 area% and 28.7 area%, respectively with the oxidized Ca-Fe oxygen carrier.[32]

In this study, value-added chemicals such as BTX, 2-pentanone as well as 2,3-dihydrobenzofuran (2,3-DHB) from corn straw biomass were prepared via chemical looping pyrolysis using either reduced or oxidized Ca-Fe composite oxygen carrier. The experimental conditions including temperature and the mass ratio of oxygen carrier to biomass (OC/B) were optimized. Furthermore, the possible mechanisms of $Ca_2Fe_2O_5$ oxygen carrier in terms of oxygen-carrying and catalysis on the production of value-added chemicals were discussed.

2 Materials and methods

2.1 *Preparation and characterization of materials*

The $Ca_2Fe_2O_5$ composite oxygen carrier for CLPy was synthesized using the sol-gel combustion method. The flow chart for the preparation of oxygen carriers is shown in Figure 1. Initially, analytically pure $Fe(NO_3)_3·9H_2O$ and $Ca(NO_3)_2·4H_2O$ (Sinopharm Chemical Reagent Co. LTD), with Fe-Ca molar ratio of 1:1 were dissolved in deionized water at room temperature. Subsequently, an appropriate amount of citric acid (Sinopharm Chemical Reagent Co. LTD), was added to the solution and stirred until complete dissolution. The resulting mixture was then transferred to a thermostatic oil bath and stirred at 90 °C until a viscous gel formed. The gel obtained was subsequently dried in an oven at 100 °C, followed by two stages of calcination in a muffle furnace: first at 300 °C for 1 h and then at 900 °C for 5 h. Finally, the samples were cooled to room temperature, crushed, sieved, and labeled as Ox-OC to indicate the oxidized oxygen carrier. To obtain the reduced oxygen carrier named Re-OC, the $Ca_2Fe_2O_5$ composite oxygen carrier was reduced by hydrogen at 850 °C for half an hour. The oxygen carrier was replaced by quartz sand in the term of control experiments.

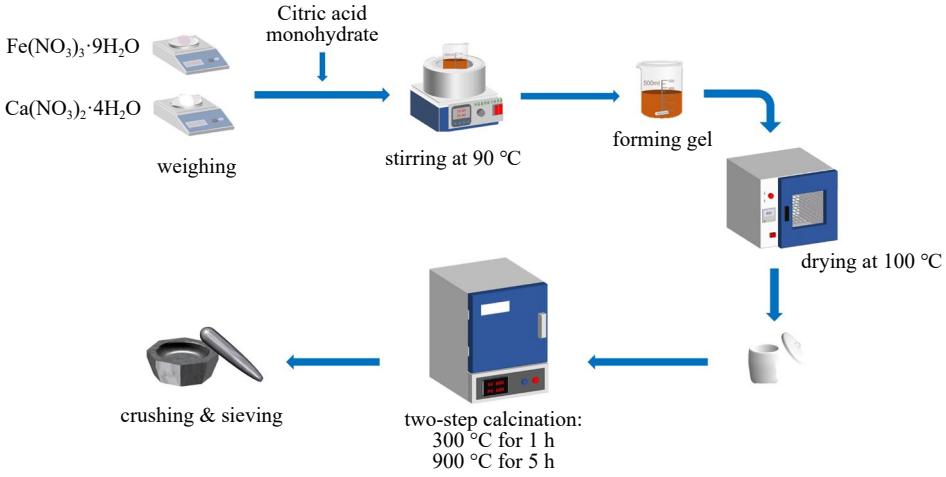

Figure 1. Flow chart for the preparation of calcium and iron oxygen carriers

The corn straws were sourced from Lianyungang, Jiangsu Province, China. After being dried for 24 hours at 105 °C, the samples were subsequently ground to obtain particles with size less than 100 μm. Proximate analysis, ultimate analysis, and chemical component analysis results are presented in Table 1. Among them, the ultimate analysis of carbon, hydrogen, nitrogen and sulfur was obtained by an elemental analyzer (Elementar UNICUBE), with the content of oxygen calculated by subtraction method. Proximate analysis was conducted using a thermogravimetric analyzer (NETZSCH STA409 PC). Component analysis was performed according to the Laboratory Analytical Procedure (LAP) of National Renewable Energy Laboratory (USA). The high oxygen content of bio-oil can be attributed to its oxygen content of 55%. Additionally, corn straws mainly consist of three key components: lignin, cellulose and hemicellulose.

Table 1. Characterization of biomass corn straws

Ultimate analysis wt.%, daf					Proximate analysis wt.%, ad				Chemical component wt.%		
C	H	O*	N	S	Moisture	Volatile	Ash	Fixed carbon	cellulose	hemicellulose	lignin
38.65	4.51	55.07	1.38	0.39	3.72	66.35	11.73	18.19	31.63	13.90	14.68

* by difference

The composition of the fresh, reduced, and reacted oxygen carrier was analyzed using an X-ray diffractometer (RigakuD-MAX2500/PC) with a Cu-Kα radiation source at a diffraction angle (2θ) ranging from 10° to 80°. All X-ray diffraction patterns were analyzed using Jade7.5 software by MDI. The surface morphology of the oxygen carrier was characterized using a scanning electron microscope (ZeissSigma500, Germany), and the elemental distribution on the surface was analyzed using an energy scattering spectrometer (Xplore).

2.2 *Experimental setup and procedure*

The experimental setup primarily consists of a heating furnace, a quartz tube reactor (600 mm × 46 mm), and product collection sets, as illustrated in Figure 2. Before carrying out the pyrolysis experiments, argon gas was purged at a flow rate of 200 mL/min for 30 min to ensure an inert atmosphere. the quartz tube reactor was heated from room temperature to the predetermined temperature (450 °C, 500 °C, 550 °C, 600 °C and 650 °C) using the heating furnace under an argon gas protective environment. Once stabilized at each temperature, a mixed sample comprising of corn straw (3 g) and oxygen carrier (1-6 g) was rapidly introduced into the heated constant temperature zone at the upper end of the reactor. Liquid products were collected by absorption bottles containing quantitative isopropyl alcohol while pyrolysis gases were collected by gasbags. Each pyrolysis experiment lasted for thirty minutes. Liquid products were dried using anhydrous sodium sulfate and filtered through Polytetrafluoroethylene (PTFE) filters with a pore size of 45 μm prior to Gas chromatography-mass spectrometry (GC-MS) analysis. Upon completion of the reaction, the reactant was transferred away from the heating zone, and subsequently cooled gradually to ambient temperature under protective atmospheres provided by argon flows.

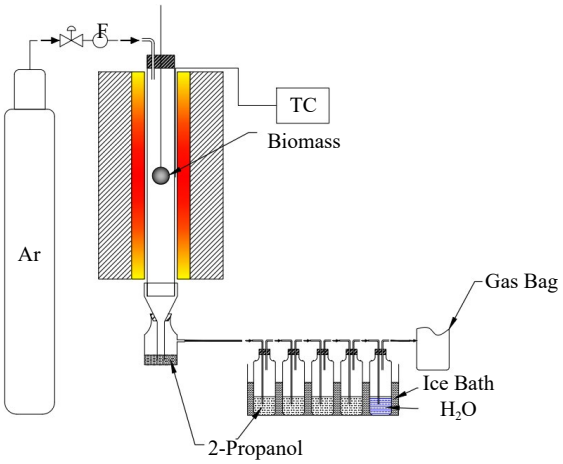

Figure 2. Diagram of the experimental setup for CLPy process of corn straws

The liquid products were analyzed using gas chromatography-mass spectrometry (7890A-5975C, Agilent, USA) equipped with an HP-5 ms column (60 m × 0.25 mm × 0.25 μm). High purity nitrogen was used as the carrier gas at a flow rate of 1 cm^3/min. The oven temperature was initially set at 80 °C and then ramped up to 280 °C at a heating rate of 10 °C/min, followed by a hold time of 15 min. The split ratio was maintained at 1:5.

3. Results and discussions

3.1 *Characterization of fresh Ca-Fe oxygen carrier*

The X-ray diffraction (XRD) patterns of the fresh Ca-Fe oxygen carriers in their oxidation state and the reduced Ca-Fe oxygen carrier by H_2 are presented in Figure 3(a) and 3(b), respectively. It is evident that the sol-gel method successfully yielded brownmillerite structured $Ca_2Fe_2O_5$ oxygen carriers, consistent with previous literature.[33] Upon

reduction at 850 °C using H_2, the oxidized Ca-Fe oxygen carrier was transformed into a mixture of CaO and Fe phases without any other valence states of iron. Scanning electron microscope and energy dispersive spectrometer (SEM-EDS) analysis in Figure 4 reveals an excellent porous structure with a uniform distribution of both calcium and iron elements for both oxidized and reduced oxygen carriers, which facilitates subsequent redox catalytic pyrolysis reactions.

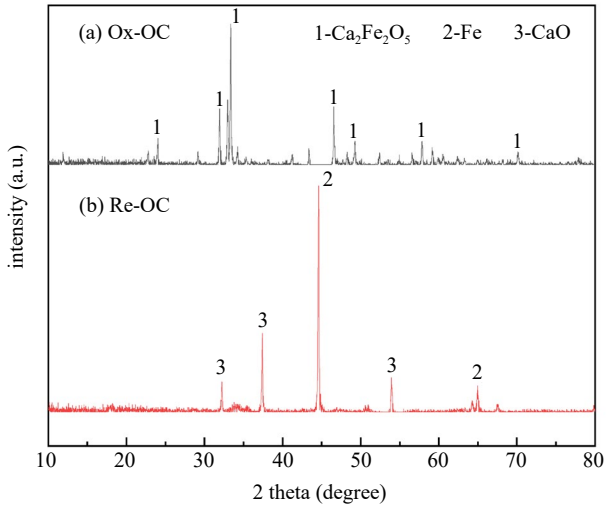

Figure 3. XRD pattern of fresh oxygen carriers. (a) Ox-OC; (b) Re-OC

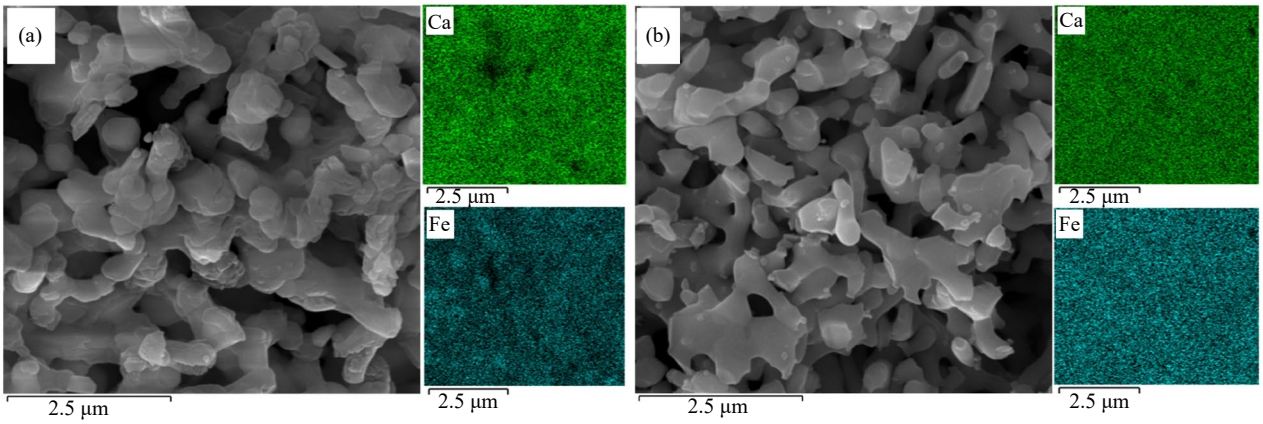

Figure 4. SEM-EDS pattern of fresh oxygen carriers. (a) Ox-OC; (b) Re-OC

3.2 *Effect of oxygen carrier on the composition of liquid products*

The total ion chromatogram of GC-MS analysis for the pyrolysis bio-oils at 600 °C is presented in Figure 5. It is evident that the predominant composition of liquid products undergoes significant changes in the presence of both oxidized and reduced Ca-Fe oxygen carriers. In the control experiment, acetic acid and 2-hexanol are identified as the main components of pyrolysis bio-oils, accounting for approximately 28.5 area% and 25.3 area%, respectively. Furthermore, phenol compounds derived from lignin component of corn straws are identified as primary aromatics. When using the reduced oxygen carrier, carboxylic acids decrease significantly with acetic acid reducing to only 11.0 area% relative percentage. Conversely, hydrocarbons such as benzene and toluene are generated, which aligns with previous literature on the deoxygenation effect of Ca-Fe oxygen carriers.[29] Additionally, there is a substantial increase in the production of 2-pentanone with its relative percentage reaching around 16.5 area%, which can be attributed to

ketonization reactions involving carboxylic acids.[30] When using the oxidized oxygen carrier, there is a decrease in relative percentage for acetic acid while promoting formation of 2-pentanone. Notably, dihydrobenzofuran (2,3-DHB), an aromatic compound with a high relative percentage (11.6%), emerges due to catalytic effects exerted by the oxidized oxygen carrier. Consequently, it can be concluded that both reduced and oxidized oxygen carriers facilitate generation of various value-added chemicals via chemical looping schemes; however further optimization of experimental conditions should be conducted.

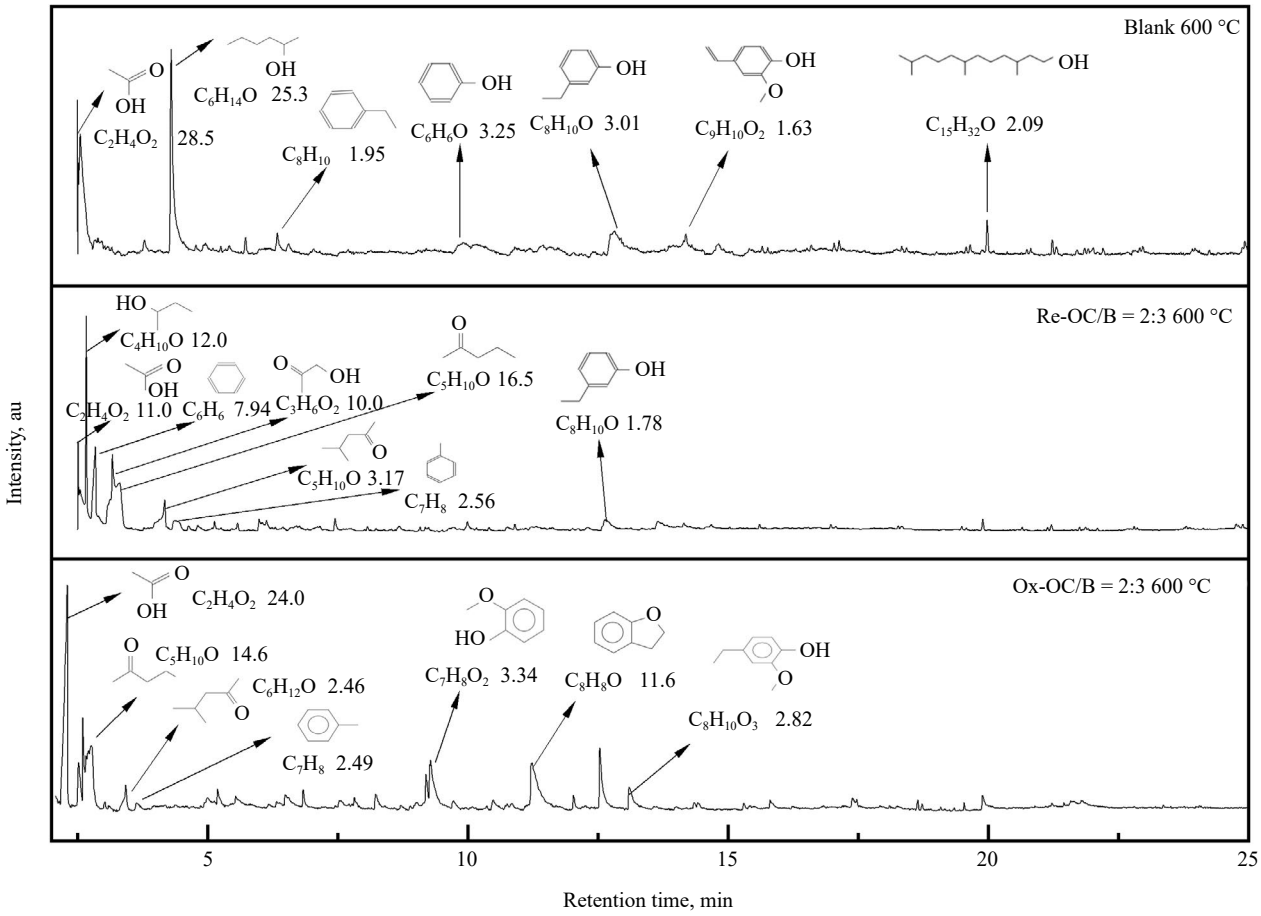

Figure 5. Total ion chromatogram of GC-MS analysis for the pyrolysis bio-oils at 600 °C. (a) without oxygen carrier; (b) with the reduced oxygen carrier; (c) with the oxidized oxygen carrier

3.3 *Preparation of BTX and 2-pentanone over the reduced oxygen carrier*

According to the pre-experiment results, the main influencing factors of oxygen carrier on the composition distribution of liquid products are pyrolysis temperature and the mass ratio of oxygen carrier to biomass, i.e. OC/B mass ratio. The impact of these two factors on the composition distribution of hydrocarbons and carboxylic acids is depicted in Figure 6. When the Re-OC/B mass ratio equals to 2:3, there is a gradual increase in the relative percentage of hydrocarbons with rising temperature, while that of carboxylic acids decreases. At 650 °C, hydrocarbons account for up to 40.8 area%, whereas carboxylic acids decrease to 7.29 area%. These findings indicate excellent deoxygenation capabilities of reduced Ca-Fe oxygen carrier. Figure 6b demonstrates the effects of Re-OC/B mass ratio on the composition distribution of hydrocarbons and carboxylic acids at their optimal temperature. It can be observed that as Re-OC/B mass ratio increases from 0 to 2:3, there is an increase in hydrocarbon distribution followed by slight changes. Conversely, carboxylic acid distribution decreases to zero as Re-OC/B mass ratio rises from 0 to 6:3. Clearly, reduced

oxygen carriers contribute significantly towards biofuel and hydrocarbon chemical production.

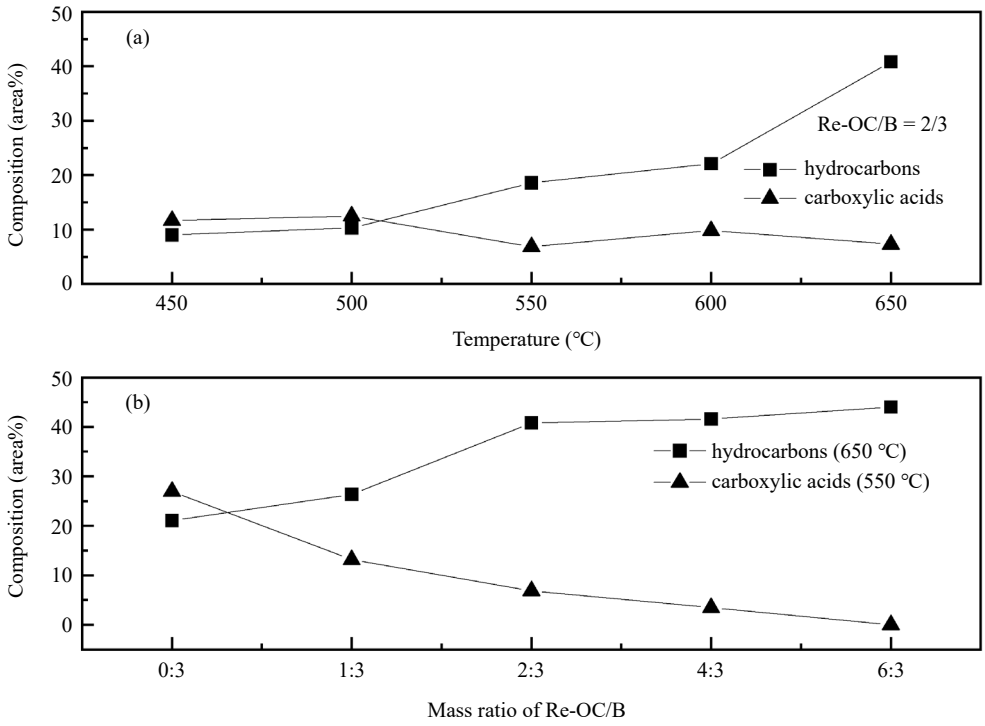

Figure 6. Composition distribution of hydrocarbons and carboxylic acids under different conditions. (a) temperature; (b) Re-OC/B mass ratio

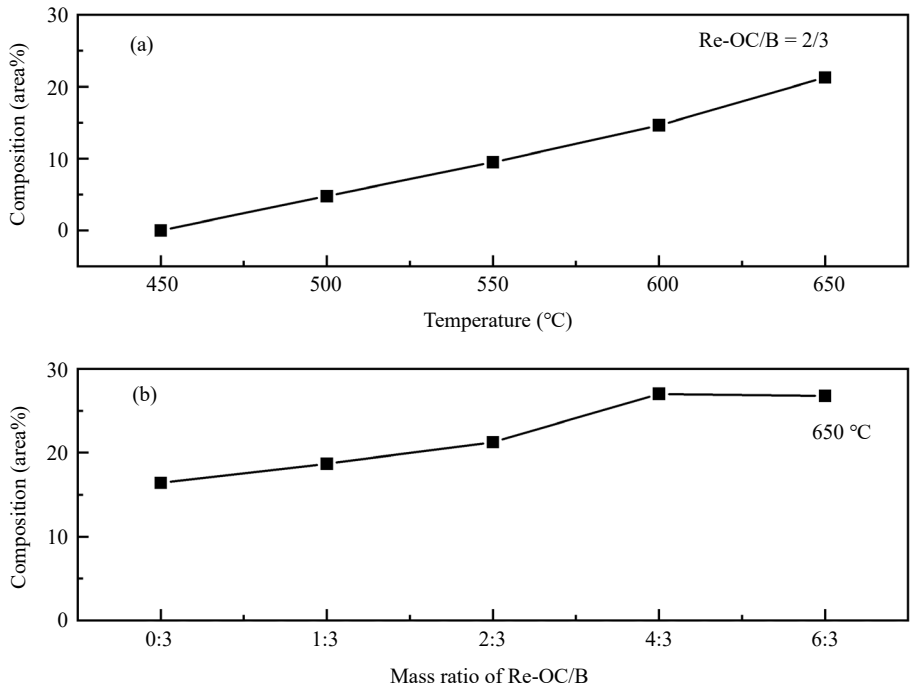

Figure 7. Composition distribution of BTX under different conditions. (a) temperature; (b) Re-OC/B mass ratio

Among hydrocarbons, benzene, toluene, and xylene (BTX) plays a pivotal role as a crucial chemical raw material for the production of various chemicals including polyethylene terephthalate (PET), aniline, nylon, and styrene. Biomass has been widely recognized as an appealing option alternative renewable feedstock for generating BTX.[34] Therefore, the generation of BTX via CLPy of corn straw was investigated. The effect of temperature and Re-OC/B mass ratio on the composition distribution of pyrolysis liquid product is illustrated in Figure 7. It was observed that at a Re-OC/B mass ratio of 2:3, there was an increase in relative percentage of BTX with increasing temperature. The maximum percentage of BTX was up to 21.3 area% at 650 °C. Furthermore, the increasing Re-OC/B mass ratio resulted in higher relative percentages of BTX with a peak value of 27.0 area% at a Re-OC/B mass ratio of 4:3. On one hand, steam reacts with reduced oxygen carrier to provide abundant hydrogen for hydrodeoxygenation during deep deoxygenation process of lignin-derived pyrolysis products, leading to substantial production of BTX over reduced oxygen carrier. On the other hand, oxidized Ca-Fe oxygen carrier facilitates catalytic aromatization reactions due to its regeneration into $Ca_2Fe_2O_5$ during pyrolysis.

2-pentanone is the other value-added chemical during the CLPy of corn straw with the reduced Ca-Fe oxygen carrier consisting of CaO and Fe. Due to its electrophilic and nucleophilic functionalities, as well as its suitable carbon chain length, 2-pentanone can be utilized for synthesizing infrastructure-compatible hydrocarbon fuels (e.g., jet fuel and diesel), lubricants, and fuel blendstocks.[35] Figure 8 illustrates the influence of temperature and Re-OC/B mass ratio on the relative percentage of 2-pentanone. It is observed that an optimal pyrolysis temperature of 550 °C leads to maximum production of 2-pentanone. Lower temperatures weaken the catalytic activity of the reduced Ca-Fe oxygen carrier, while higher temperatures accelerate cracking reactions of 2-pentanone. Regarding the effect of Re-OC/B mass ratio, an optimal value is achieved with a ratio of 4:3 when operating below 550 °C; however, this changes to a ratio of 1:3 when operating at higher temperatures (550 °C, 600 °C, and 650 °C). The highest relative percentage (38.0 area%) occurs at conditions with a temperature of 550 °C and Re-OC/B mass ratio of 1:3, respectively. According to the varying percentage of carboxylic acids discussed in the preceding section, the formation of 2-pentanone is likely attributed to the ketonization process of acetic acid, this is because both CaO and $Ca_2Fe_2O_5$ serve as catalysts for ketonization reactions. CaO acts as a bulk catalyst through thermal decomposition of calcium acetate formed, while $Ca_2Fe_2O_5$ catalyzes ketonization reactions via a redox mechanism.[36-37]

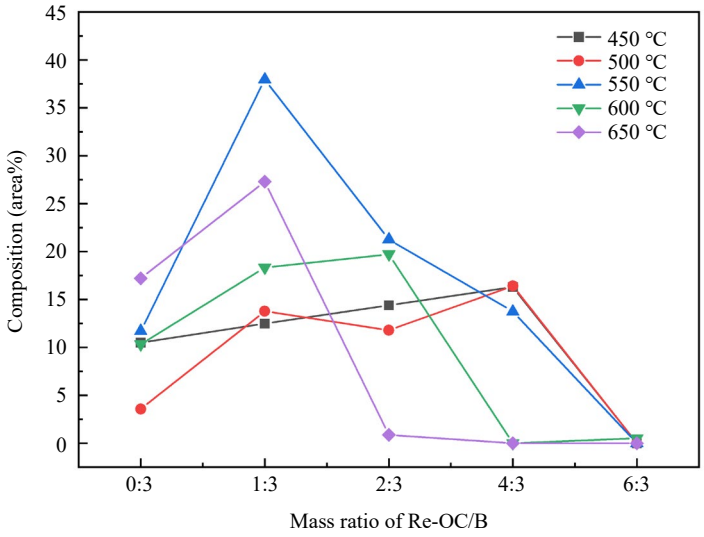

Figure 8. Composition distribution of 2-pentanone under different conditions

Furthermore, the amount of the produced 2-pentanone was further quantified by performing calibration using external standard method based on GC-MS analysis. As shown in Figure 9, a standard curve of 2-pentanone was obtained under identical test conditions. Based on this calibration curve, it was determined that the yield of 2-pentanone reached up to 4.7 wt.% on the basis of corn straws.

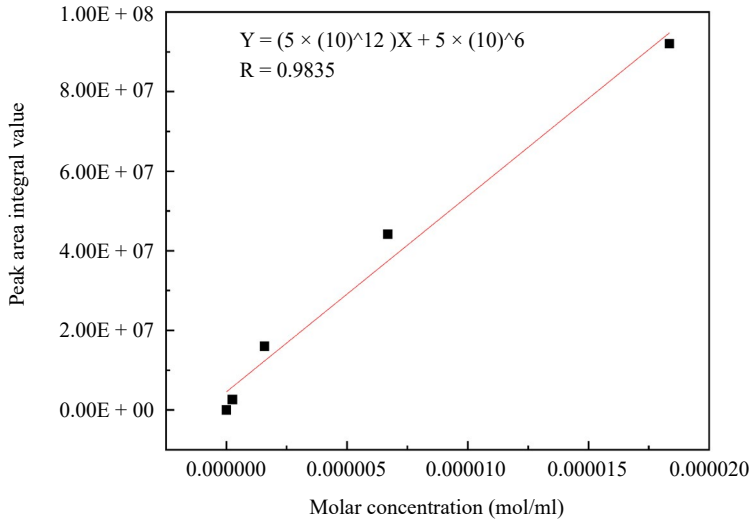

Figure 9. Standard curve of 2-pentanone

3.4 *Preparation of 2,3-DHB and 2-pentanone over the oxidized oxygen carrier*

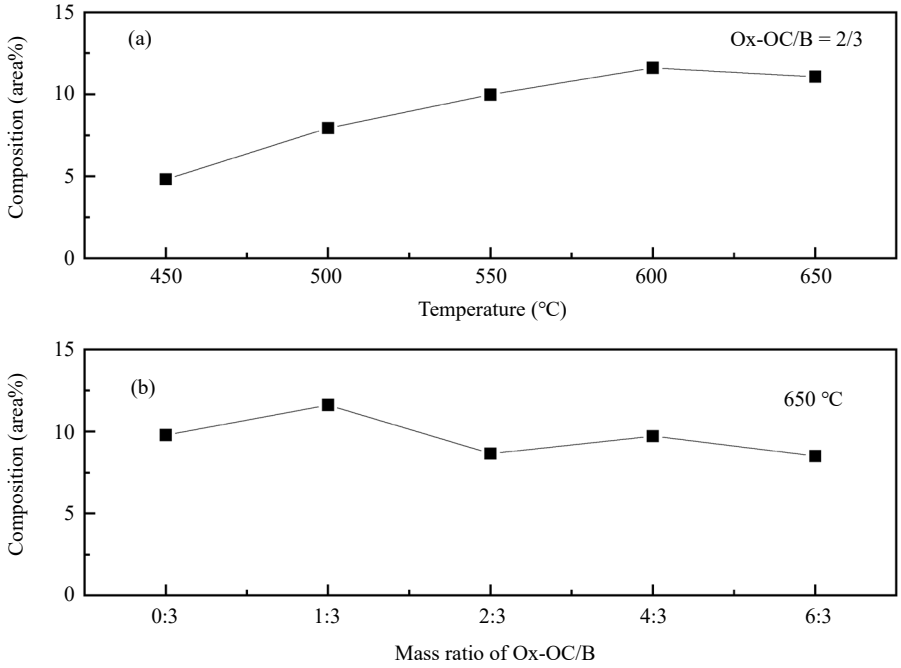

Figure 10. Composition distribution of 2,3-DHB under different conditions. (a) temperature; (b) mass ratio of Ox-OC/B

According to the experimental results in section 3.2, the dominant compositions observed over the oxidized Ca-Fe oxygen carrier were identified as 2,3-DHB and 2-pentanone. Due to their unique structures and biological activities, 2,3-DHB natural products from various plant species have attracted the interest of synthetic chemists.[38] Optimization experiments via a chemical looping scheme were conducted for both dominant compositions under different operating conditions. The effect of temperature and Ox-OC/B mass ratio on the relative percentage of 2,3-DHB is demonstrated in Figure 10. It was observed that with increasing temperature from 450 °C to 600 °C, there was a subsequent slight decrease at 650 °C in the relative percentage of 2,3-DHB. Additionally, Figure 10b illustrates that variations in Ox-OC/

B mass ratio had minimal impact on the relative percentage of this compound. Consequently, it was determined that an optimal condition could be achieved with an Ox-OC/B mass ratio of 2:3 at 600 °C. The maximum value reaches 11.6 area% at these optimal conditions. The generation of 2,3-DHB occurs through the pyrolysis of lignin component in corn straw with catalytic assistance from oxidized Ca-Fe oxygen carriers; however further investigation is required to elucidate the underlying catalytic mechanism. Significantly, CLPy introduces an innovative methodology for synthesizing 2,3-DHB obtained from corn straw.

Figure 11 illustrates the impact of temperature and Ox-OC/B mass ratio on the relative percentage of 2-pentanone in the presence of an oxygen carrier. It is observed that the relative percentage of 2-pentanone increases as the temperature decreases and the Ox-OC/B mass ratio increases. The highest relative percentage (28.0 area%) occurs at conditions with a Re-OC/B mass ratio of 4:3 at 450 °C. Compared to the reduced oxygen carrier, there is a decrease in the relative percentage of 2-pentanone at optimal conditions due to the absence of CaO catalysis on ketonization reaction of carboxylic acids. Additionally, hydrocarbon production decreases because there is no hydrogen atmosphere generated through reaction between reduced oxygen carrier and steam.

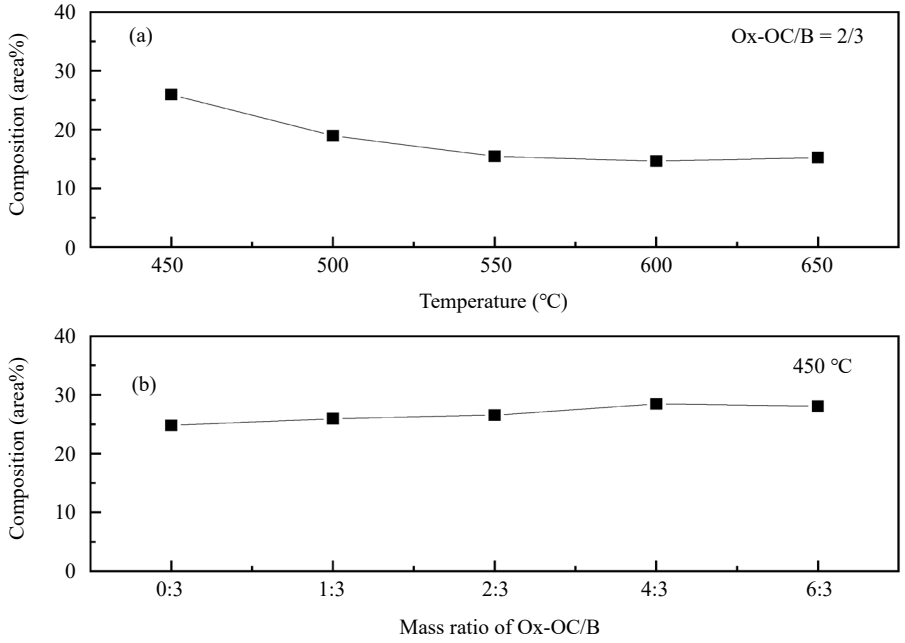

Figure 11. Composition distribution of 2-pentanone under different conditions. (a) temperature; (b) mass ratio of Ox-OC/B

3.5 *Oxygen-carrying and catalytic function of $Ca_2Fe_2O_5$ oxygen carrier*

According to the principle of CLPy, the oxygen carrier serves dual functions, i.e. oxygen-carrying and catalyst. In the term of oxygen-carrying function, oxygen donors refer to providing lattice oxygen for gasifying biomass or biochar in the form of oxidized oxygen carrier, while oxygen acceptor represents either deoxygenation of bio-oil during biomass pyrolysis or capturing molecule oxygen from air using reduced oxygen carrier. Regarding its catalytic function, it involves facilitating specific chemical composition during biomass pyrolysis or promoting the gasification of bio-char into syngas.

The XRD characterization of Ca-Fe oxygen carriers in different oxidation states under various optimization conditions is illustrated in Figure 12. It was observed that, after the pyrolysis process, a portion of the reduced oxygen carrier underwent re-oxidation to form $Ca_2Fe_2O_5$. Due to insufficient availability of oxygen during pyrolysis, only a fraction of $Ca_2Fe_2O_5$ was formed. Furthermore, due to the reaction between CO_2 produced during pyrolysis and CaO, the presence of $CaCO_3$ was also in solid products after pyrolysis. Both $Ca_2Fe_2O_5$ and $CaCO_3$ indicated its deoxygenation function to the pyrolysis of corn straw. Meanwhile, the generated $Ca_2Fe_2O_5$ could regulate the composition of pyrolysis

product as a catalyst. As shown in Figure 12b, with respect to the oxidation state of the oxygen carrier for corn straw pyrolysis, there is no change in its crystal structure after the pyrolysis reaction. This suggests that the primary function of the oxygen carrier lies in catalytic conversion to 2-pentanone and 2,3-DHB.

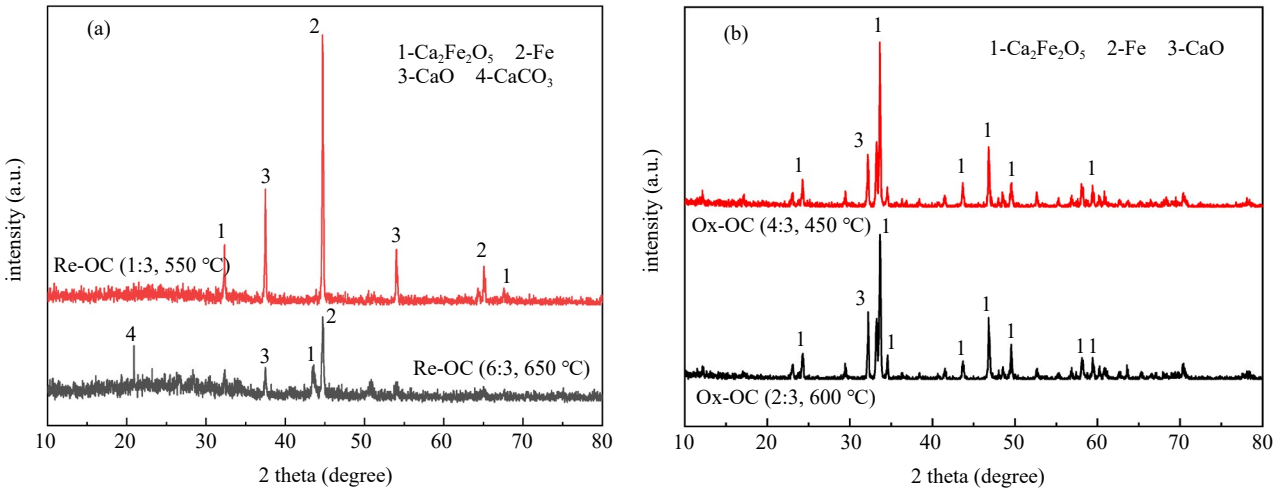

Figure 12. XRD pattern of oxygen carriers after pyrolysis. (a) Reduced OC; (b) Oxidized OC

SEM-EDS images of oxygen carriers after pyrolysis under various optimization conditions are shown in Figure 13. It can be observed that the reacted oxygen carrier maintains excellent surface morphology and spatial structure, with even distribution of Ca, Fe and O elements. Clearly, a carbon layer covers the reacted oxygen carrier due to the formation of bio-char, which can be eliminated through gasification reaction with inherent oxygen or extrinsic gasifying agents.[29-31]

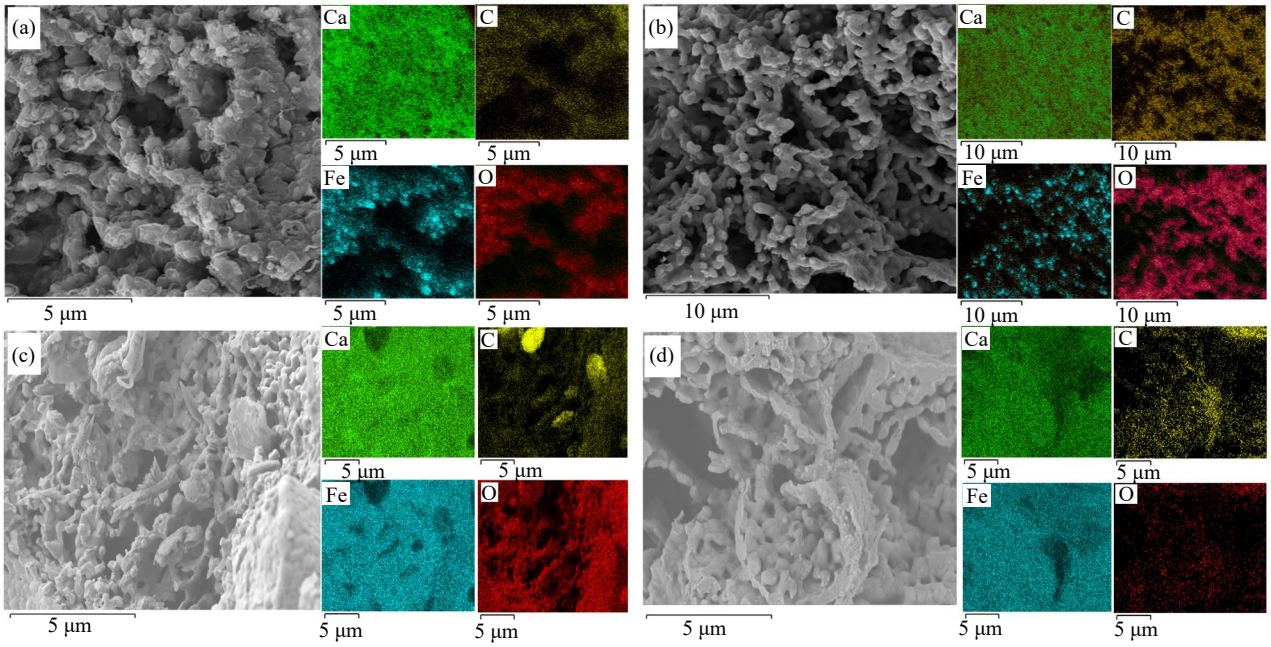

Figure 13. SEM-EDS images of oxygen carriers after pyrolysis. (a) Re-OC/B = 1:3, T = 550 °C, (b) Re-OC/B = 4:3 650 °C, (c) Ox-OC/B = 2:3, T = 600 °C, and (d) Ox-OC/B = 4:3, T = 450 °C

4. Conclusions

In this study, a chemical looping pyrolysis approach was employed to produce value-added chemicals using both reduced and oxidized Ca-Fe oxygen carriers. The effect of temperature and the mass ratio of oxygen carrier to biomass (OC/B) on the production of value-added chemicals such as BTX, 2-pentanone, and 2,3-dihydrobenzofuran (2,3-DHB) from corn straw biomass was investigated.

It was found that the reduced Ca-Fe oxygen carrier promotes the formation of hydrocarbons and facilitates the removal of oxygenated compounds in bio-oil. Under optimal conditions (Re-OC/B = 4:3, T = 650 °C), the relative percentage of BTX reaches 27.0 area%. The catalytic ketonization of both CaO and $Ca_2Fe_2O_5$ leads to a significant increase in 2-pentenone, accounting for 38.0 area% or equivalently 4.7 wt.% based on corn straws.

As for the oxidized Ca-Fe oxygen carrier, the relative percentage of 2,3-DHB reached a maximum of 11.6% at 600 °C with an Ox-OC/B mass ratio of 2:3. Additionally, a lower temperature of 450 °C is conductive to the generation of 2-pentenone. Under catalytic ketonization using an oxidized Ca-Fe oxygen carrier, a maximum value of 28.0 area% was achieved with an Ox-OC/B mass ratio of 4:3.

This study not only demonstrates the feasibility of chemical looping pyrolysis conversion for lignocellulosic biomass but also presents a novel approach for the efficient conversion and utilization of agricultural straws. Further research is required for the multiple redox-cycle performance.

Acknowledgements

The authors gratefully acknowledge the financial support from the Talent Fund of Shandong Collaborative Innovation Center of Eco-Chemical Engineering (Grant No. XTCXQN06).

Conflict of interest

The authors declare no competing financial interest.

References

[1] Qiu, Y.; Zhong, D.; Zeng, K.; Li, J.; Yang, H.; Chen, H. Evolution of lignin pyrolysis heavy components through the study of representative lignin monomers. *Fuel Process. Technol*. **2023,** *250*, 107910.
[2] Xu, Z.; Tang, Y.; Wang, Q.; Xu, Y.; Yuan, X.; Ma, Q.; Wang, G.; Liu, M.; Hao, H. Emergy based optimization of regional straw comprehensive utilization scheme. *J. Cleaner Prod*. **2021,** *297*, 126638.
[3] Fu, Y.; Zhang, J.; Guan, T. High-value utilization of corn straw: from waste to wealth. *Sustainability* **2023,** *15*, 14618.
[4] Isinkaralar, K.; Nurmakova, S. M. Does agricultural biomass matter for environmental sustainability? Enhanced adsorption capacity of BTEX mixture using powdered activated carbon by agricultural biomass. *Biomass Conv. Bioref*. **2023**. https://doi.org/10.1007/s13399-023-04990-4.
[5] Isinkaralar, K. Multi-component volatile organic compounds (VOCs) treatment nexus: High-performance of activated carbon derived from residual agroforestry biomass. *Int. J. Environ. Sci. Technol*. **2024,** *21*, 925-938.
[6] Goyal, H. B.; Seal, D.; Saxena, R. C. Bio-fuels from thermochemical conversion of renewable resources: a review. *Renew. Sust. Energ. Rev*. **2008,** *12*, 504-517.
[7] Wang, S.; Dai, G.; Yang, H.; Luo, Z. Lignocellulosic biomass pyrolysis mechanism: A state-of-the-art review. *Prog. Energ. Combust*. **2017,** *62*, 33-86.
[8] Dai, L.; Wang, Y.; Liu, Y.; He, C.; Ruan, R.; Yu, Z.; Jiang, L.; Zeng, Z.; Wu, Q. A review on selective production of value-added chemicals via catalytic pyrolysis of lignocellulosic biomass. *Sci. Total Environ*. **2020,** *749*, 142386.
[9] Yildiz, G.; Ronsse, F.; van Duren, R.; Prins, W. Challenges in the design and operation of processes for catalytic fast pyrolysis of woody biomass. *Renew. Sust. Energ. Rev*. **2016,** *57*, 1596-1610.
[10] Sekar, M.; Mathimani, T.; Alagumalai, A.; Chi, N. T. L.; Duc, P. A.; Bhatia, S. K.; Brindhadevi, K.; Pugazhendhi, A.

A review on the pyrolysis of algal biomass for biochar and bio-oil-bottlenecks and scope. *Fuel* **2021,** *283*, 119190.
[11] Jin, W.; Pastor-Perez, L.; Shen, D. K.; Sepulveda-Escribano, A.; Gu, S.; Reina, T. R. Catalytic upgrading of biomass model compounds: novel approaches and lessons learnt from traditional hydrodeoxygenation-a review. *ChemCatChem* **2019,** *11*, 924-960.
[12] Liu, R.; Sarker, M.; Rahman, M. M.; Li, C.; Chai, M.; Cotillon, R.; Scott, N. R. Multi-scale complexities of solid acid catalysts in the catalytic fast pyrolysis of biomass for bio-oil production-a review. *Prog. Energ. Combust*. **2020,** *80*, 100852.
[13] Chen, Y. K.; Lin, C. H.; Wang, W. C. The conversion of biomass into renewable jet fuel. *Energy* **2020,** *201*, 117655.
[14] Lahijani, P.; Mohammadi, M.; Mohamed, A. R.; Ismail, F.; Lee, K. T.; Amini, G. Upgrading biomass-derived pyrolysis bio-oil to bio-jet fuel through catalytic cracking and hydrodeoxygenation: A review of recent progress. *Energy Convers. Manage*. **2022,** *268*, 115956.
[15] Zhang, H.; Yang, K.; Tao, Y.; Yang, Q.; Xu, L.; Liu, C.; Ma, L.; Xiao, R. Biomass directional pyrolysis based on element economy to produce high-quality fuels, chemicals, carbon materials-a review. *Biotechnol. Adv*. **2023,** *69*, 108262
[16] Doroshenko, A.; Pylypenko, I.; Heaton, K.; Cowling, S.; Clark, J.; Budarin, V. L. Selective microwave-assisted pyrolysis of cellulose towards Levoglucosenone using clay cata lysts. *ChemSusChem* **2019,** *12*, 5224-5227.
[17] Taimoor, A. A.; Favre-Réguillon, A.; Vanoye, L.; Pitault, I. Upgrading of biomass transformation residue: influence of gas flow composition on acetic acid ketonic condensation. *Catal. Sci. Technol*. **2012,** *2*, 359-363.
[18] Sweygers, N.; Depuydt, D. E. C.; Van Vuure, A. W.; Degrève, J.; Potters, G.; Dewil, R.; Appels, L. Simultaneous production of 5-hydroxymethylfurfural and furfural from bam boo (Phyllostachys nigra "Boryana") in a biphasic reaction system. *Chem. Eng. J*. **2020,** *386*, 123957.
[19] Zhang, Y.; Lei, H.; Yang, Z.; Qian, K.; Villota, E. Renewable high-purity mono-phenol production from catalytic microwave-induced pyrolysis of cellulose over biomass derived activated carbon catalyst. *ACS Sustain. Chem. Eng*. **2018,** *6*, 5349-5357.
[20] Cao, L.; Yu, I. K. M.; Liu, Y.; Ruan, X.; Tsang, D. C. W.; Hunt, A. J.; Ok, Y. S.; Song, H.; Zhang, S. Lignin valorization for the production of renewable chemicals: state of the art review and future prospects. *Bioresour. Technol*. **2018,** *269*, 465-475.
[21] Gutierrez, A.; Kaila, R. K.; Honkela, M. L.; Slioor, R.; Krause, A. O. I. Hydrodeoxygenation of guaiacol on noble metal catalysts. *Catal. Today* **2009,** *147*, 239-246.
[22] Bulushev, D. A.; Ross, J. R. H. Catalysis for conversion of biomass to fuels via pyrolysis and gasification: A review. *Catal. Today* **2011,** *171*, 1-13.
[23] Lu, Q.; Zhang, Z. F.; Dong, C. Q.; Zhu, X. F. Catalytic upgrading of biomass fast pyrolysis vapors with nano metal oxides: An analytical Py-GC/MS study. *Energies* **2010,** *3*, 1805-1820.
[24] Aysu, T.; Fermoso, J.; Sanna, A. Ceria on alumina support for catalytic pyrolysis of pavlova sp. microalgae to high-quality bio-oils. *J. Energy Chem*. **2017,** *27*, 874-882.
[25] Zheng, A.; Zhao, Z.; Chang, S.; Huang, Z.; Wu, H.; Wang, X.; He, F.; Li, H. Effect of crystal size of ZSM-5 on the aromatic yield and selectivity from catalytic fast pyrolysis of biomass. *J. Mol. Catal. A: Chem.* **2014,** *383*, 23-30.
[26] Chaihad, N.; Karnjanakom, S.; Kurnia, I.; Yoshida, A.; Abudula, A.; Reubroycharoen, P.; Guan, G. Catalytic upgrading of bio-oils over high alumina zeolites. *Renew. Energy* **2019,** *136*, 1304-1310.
[27] Che, Q.; Yang, M.; Wang, X.; Yang, Q.; Williams, L. R.; Yang, H.; Zou, J.; Zeng, Z. K.; Zhu, Y.; Chen, Y.; Chen, H. Influence of physicochemical properties of metal modified ZSM-5 catalyst on benzene, toluene and xylene production from biomass catalytic pyrolysis. *Bioresour. Technol*. **2019,** *278*, 248-254.
[28] Li, X.; Li, J.; Zhou, G.; Feng, Y.; Wang, Y.; Yu, G.; Deng, S.; Huang, J.; Wang, B. Enhancing the production of renewable petrochemicals by co-feeding of biomass with plastics in catalytic fast pyrolysis with ZSM-5 zeolites. *Appl. Catal. A* **2014,** *481*, 173-182.
[29] Liu, Y.; Liu, J.; Wang, T.; Zhang, X.; Wang, L.; Hu, X.; Guo, Q. Co-production of upgraded bio-oil and H_2-rich gas from microalgae via chemical looping pyrolysis. *Int. J. Hydrogen Energ*. **2021,** *46*, 24942-24955.
[30] Liu, Y.; Wang, T.; Zhang, X.; Hu, X. D.; Liu, T.; Guo, Q. Chemical looping staged conversion of microalgae with calcium ferrite as oxygen carrier: pyrolysis and gasification characteristics. *J. Anal. Appl. Pyrol*. **2021,** *156*, 105.
[31] He, X.; Liu, J.; Li, W.; Liu, Y.; Guo, Q. Oxygen-carrying and catalytic properties of iron-based composite oxygen carrier for chemical looping pyrolysis of corn stalk. *CIESC J*. **2023,** *74*, 4153-4163.
[32] Gao, X.; He, X.; Liu, Y.; Zhang, X.; Hu, X.; Guo, Q. Chemical looping pyrolysis-gasification staged conversion of microalgae biomass with Ca-Fe composite oxygen carrier. *Int. J. Greenhouse Gas Control*. **2023,** *127*, 103941.
[33] Liu, G.; Liao, Y.; Wu, Y.; Ma, X. Application of calcium ferrites as oxygen carriers for microalgae chemical

looping gasification. *Energy Convers. Manage*. **2018,** *160*, 262-272.
[34] Wu, Y. K.; Yang, J.; Wu, G.; Gao, W. R.; Lora, E. E. S.; Isa, Y. M.; Subramanian, K. A.; Kozlov, A.; Zhang, S.; Huang, Y. Benzene, toluene, and xylene (BTX) production from catalytic fast pyrolysis of biomass: a review. *ACS Sustainable Chem. Eng*. **2023,** *11*, 11700-11718.
[35] Subramaniam, S.; Guo, M. F.; Bathena, T.; Gray, M.; Zhang, X.; Martinez, A.; Kovarik, L.; Goulas, K. A.; Ramasamy, K. K. Direct catalytic conversion of ethanol to C_{5+} ketones: role of Pd-Zn alloy on catalytic activity and stability. *Angew. Chem. Int. Ed*. **2020,** *59*, 14550-14557.
[36] Landoll, M. P.; Holtzapple, M. T. Thermal decomposition of mixed calcium carboxylate salts: effects of lime on ketone yield. *Biomass Bioenergy* **2011,** *35*, 3592-3603.
[37] Kumar, R.; Enjamuri, N.; Shah, S.; Al-Fatesh, A. S.; Bravo-Suárez, J. J.; Chowdhury, B. Ketonization of oxygenated hydrocarbons on metal oxide based catalysts. *Catal. Today* **2018,** *302*, 16-49.
[38] Chen, Z.; Pitchakuntla, M.; Jia Y. Synthetic approaches to natural products containing 2,3-dihydrobenzofuran skeleton. *Nat. Prod. Rep*. **2019,** *36*, 666-690.